

Article

# Optimization of Design Pressure Ratio of Positive Displacement Expander for Vehicle Engine Waste Heat Recovery †

Young Min Kim \*, Dong Gil Shin and Chang Gi Kim

Department of Environmental and Energy Systems, Korea Institute of Machinery & Materials, 171 Jang-dong, Yuseong-gu, Daejeon 305-343, Korea; E-Mails: sdk@kimm.re.kr (D.G.S.); cgkim@kimm.re.kr (C.G.K.)

† This article is based on a paper written in Korean and published by *Journal of Energy Engineering*, 2012, 21, 398–406.

\* Author to whom correspondence should be addressed; E-Mail: ymkim@kimm.re.kr; Tel.: +82-42-868-7377; Fax: +82-42-868-7305.

Received: 31 July 2014; in revised form: 15 September 2014 / Accepted: 16 September 2014 / Published: 22 September 2014

---

**Abstract:** This study investigated the effect of the built-in volume ratio of an expander on the performance of a dual-loop Rankine cycle system for the engine waste heat recovery of a vehicle. Varying vehicle operating conditions can cause a positive displacement expander to operate in both under- and over-expansion states. Therefore, analysis of the off-design performance of the expander is very important. Furthermore, the volume and weight of the expander must be considered in its optimization along with the efficiency. A simple modeling of the off-design operation of the expander showed that a built-in volume ratio that causes under-expansion rather than over-expansion at the target condition is more desirable.

**Keywords:** engine waste heat recovery; Rankine cycle; expander; under-expansion; over-expansion; expansion efficiency

---

## 1. Introduction

Much of the energy produced by the fuel consumed by a vehicle is wasted in the form of exhaust gas heat and engine coolant heat. Recently, much attention has been paid to technology that improves fuel efficiency in large trucks [1] and passenger cars [2–4] through the operation of a Rankine cycle

system that utilizes such engine waste heat. The most essential component in a Rankine cycle system is the expander; either a turbo-expander or positive displacement expander can be used. A positive displacement expander such as a piston or scroll expander has many advantages over the turbo-expander typically employed in small-scale Rankine cycle systems in terms of the low-speed operation characteristics, good part-load characteristics, and cost [4–6]. In general, most studies on Rankine cycle systems for engine waste heat recovery in vehicles have been based on the necessary design pressure ratios of the positive displacement expanders in order to meet certain target operating conditions [5]. However, when a positive displacement expander is applied to a car, not only the expander efficiency but also the expander size should be considered for system optimization. This is because the installation space constraint increases with the volume of the expander, which subsequently causes deterioration of the fuel efficiency because of the weight increase.

Furthermore, the engine waste heat of a vehicle can vary depending on the operating conditions, so a Rankine cycle system designed under a certain target operating condition will sometimes operate under off-design conditions. Thus, a positive displacement expander may become under-expanded (*i.e.*, the design pressure ratio is lower than the operating pressure ratio) or over-expanded (*i.e.*, the design pressure ratio is higher than the operating pressure ratio) [6]. Therefore, the design pressure ratio of a positive displacement expander for vehicle engine waste heat recovery should be based on not only the target operating condition but also the efficiency characteristics in an off-design state.

This paper presents an analysis method for optimizing the design pressure ratio of a positive displacement expander in a dual-loop mode engine waste heat recovery system that considers both the expander's expansion efficiency and its size and predicts the off-design state performance [7].

## 2. Dual-Loop Mode Engine Waste Heat Recovery System

### 2.1. System Configuration and Cycle Operating Conditions

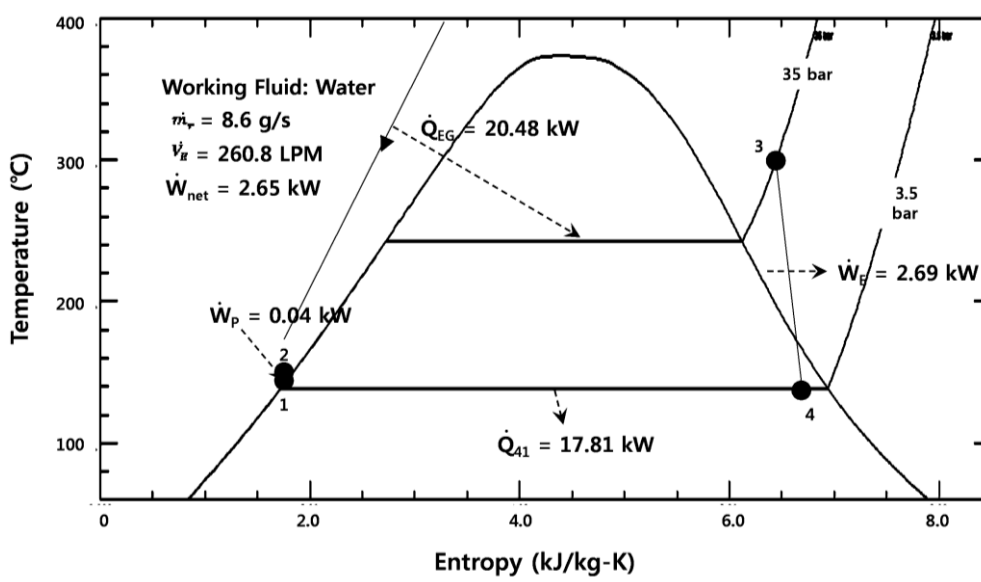
In South Korea, a dual-loop mode system that consists of a high-temperature (HT) cycle and a low-temperature (LT) cycle is currently under development for engine waste heat recovery. Dual-loop systems are desirable to obtain the maximum power output from both high- and low-temperature heat sources [1,2,8]. The HT cycle uses water as a working fluid for the heat recovery of HT exhaust gas because of its many advantages, such as no risk of decomposition, very low viscosity, high latent and specific heats, non-toxicity, non-flammability, and low cost [9]. On the other hand, the LT cycle uses R134a as a working fluid to not only recover engine coolant heat at low temperatures but also to simultaneously utilize condensation heat from the HT cycle. R134a is more suitable for low temperature (~100 °C) applications than R245fa because it can reduce the size of the expander owing to the higher operating pressure and can be replaced by R1234yf, which has similar thermodynamic properties but a very low global warming potential (GWP), for the near future. The scroll expander has many advantages, such as few parts, the ability to handle two-phase working fluids, and its inherent reliability [10]. However, the scroll expander is only used for the LT expander, not for the HT expander, because the uneven thermal deformation of the scrolls under high temperatures is difficult to handle. Therefore, a swash plate-type expander is used for the HT expander; this is suitable for HT conditions because of the simple geometry and robustness and for a high expansion ratio of about 10.

In the present study, the operating conditions of the target vehicle engine for the engine waste heat recovery system were based on a constant speed driving state of 120 km/h (engine power: 26.7 kW). The flow rate and temperature of the exhaust gas were 118 kg/h and 689 °C, respectively. Based on an air temperature of 25 °C, the exhaust heat energy, coolant flow rate, coolant outlet temperature, and engine coolant heat energy were 25.2 kW, 40 L/min, 100 °C, and 26.8 kW, respectively.

## 2.2. Target Cycle Operating Conditions and Volume of Positive Displacement Expander

In the HT cycle, the cycle efficiency increases with the maximum pressure and temperature of the steam from the exhaust gas heat  $Q_{EG}$ , as shown in Figure 1. However, because of constraints on the expander and heat exchanger design, the maximum pressure and temperature in the expander inlet were set to 35 bar and 300 °C, respectively. The cycle efficiency increases with the design expansion pressure ratio as the condensation temperature in the HT cycle  $T_{C,HT}$  decreases, but the size of the swash plate-type expander also increases. In a previous study [11], decreasing  $T_{C,HT}$  from 139 to 120 °C and then 105 °C caused the HT cycle power to increase by about 21% and 38%, respectively, although the LT cycle power was constant. However, the volume of the HT expander had to be increased by approximately 67% and 165%, respectively, to achieve this, which is a disadvantage. In the present study, therefore, the design pressure ratio was set to 10 in consideration of the size of the swash plate-type expander in the HT cycle under the target cycle operating conditions, and the condensation pressure and temperature were set to 3.5 bar and 139 °C, respectively.

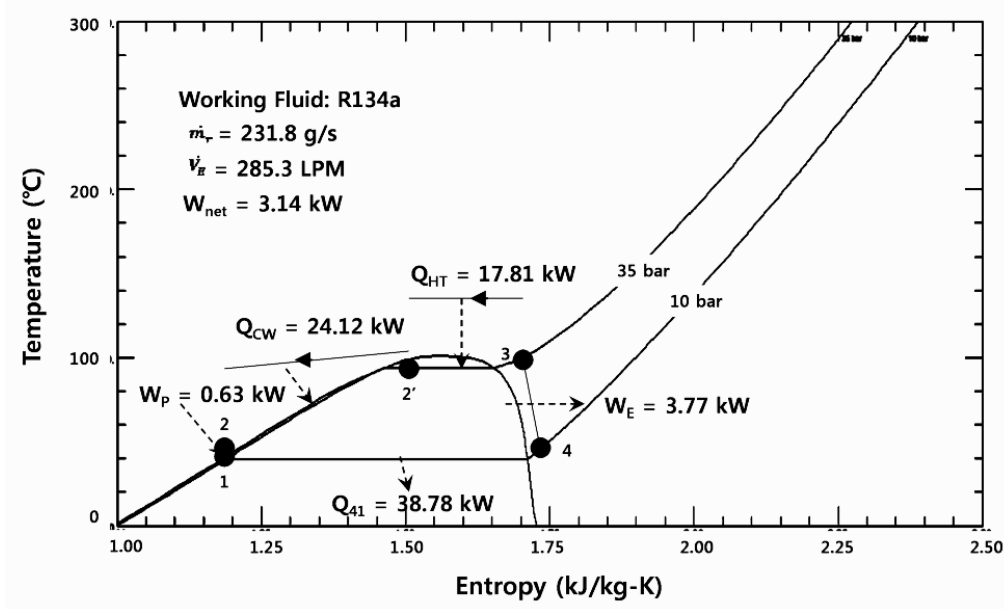
**Figure 1.** Temperature–entropy diagram of the high-temperature (HT) cycle.



In the LT cycle, the evaporation temperature was set to 93.7 °C to provide an evaporation pressure of 35 bar to utilize the engine coolant heat  $Q_{CW}$  at a temperature of 100 °C, as shown in Figure 2. In addition, the temperature of the superheated working fluid in the expander inlet, which was heated by receiving the heat  $Q_{HT}$  from the HT cycle, was set to 100 °C. Similar to the HT cycle, the cycle efficiency improves as the LT condensation temperature  $T_{C,LT}$  decreases, but this causes the LT expander volume to increase.  $T_{C,LT}$  can vary considerably depending on both the outdoor temperature

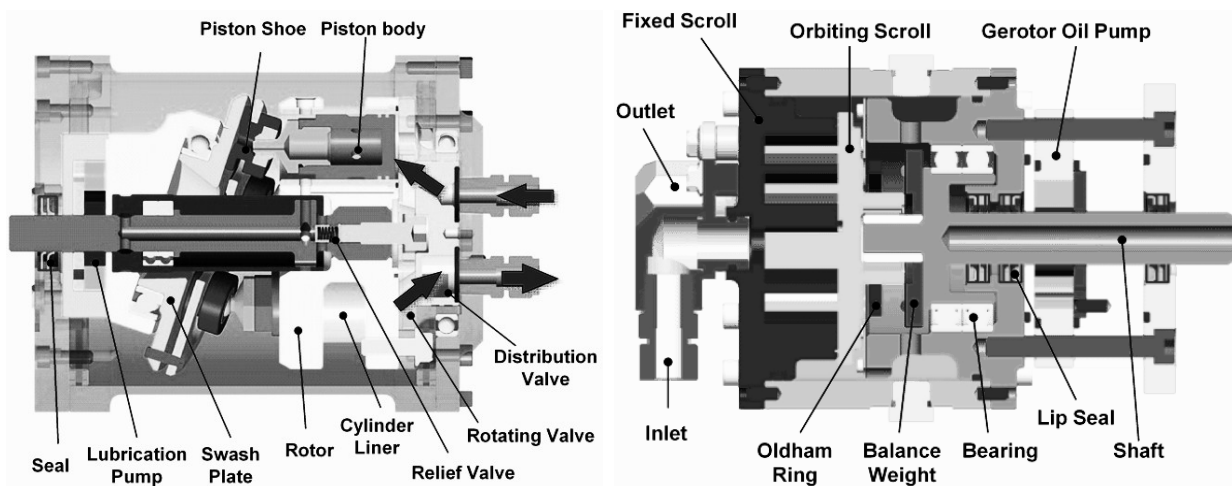
of the air-cooled condenser and the heat exchanger performance. In this study, a  $T_{C,LT}$  of 40 °C (condensation pressure: 10.2 bar) was set as a target operating condition based on the mean air temperature of all four seasons, which is 15 °C.

**Figure 2.** Temperature–entropy diagram of the low-temperature (LT) cycle.



Although the high pressure of 35 bar in the HT and LT cycles for a vehicle requires increased safety measures because it is about twice the maximum pressure of current air conditioning systems, it is necessary to achieve high efficiency. Figure 3 shows cross-section diagrams of the swash plate-type expander in the HT cycle and scroll expander in the LT cycle. In the swash plate-type expander, the piston has a diameter of 30.2 mm and five cylinders. The displacement volume is 108 cm<sup>3</sup>, and the rated driving speed is 2450 rpm. For the scroll expander, the displacement volume at the outlet is 40 cm<sup>3</sup>, and the rated driving speed is 3600 rpm.

**Figure 3.** Swash plate-type expander for the HT cycle and scroll expander for the LT cycle.



### 3. Expansion Characteristics of Positive Displacement Expander under Off-Design Operating Conditions

#### 3.1. Under-Expansion and Over-Expansion

Figure 4 shows a pressure–volume (P–V) diagram to illustrate the isentropic expansion process in the positive displacement expander, where  $P_i$ ,  $P_d$ , and  $P_e$  represent the expander supply (inlet) pressure, design expansion pressure, and operating expansion (exit) pressure, respectively. When the design pressure ratio  $P_i/P_d$  is less than the operating pressure ratio  $P_i/P_e$ , under-expansion occurs. Over-expansion occurs when  $P_i/P_d$  is higher than  $P_i/P_e$ . Upon under-expansion, a loss of available work as large as the area of region  $A_{3,u}$  occurs due to blow-down when the expansion valve (or pocket) is opened. Upon over-expansion, a loss occurs because negative work is performed over an area as large as the  $A_{3,o}$  region due to the backflow caused by back pressure when the expansion valve is opened. This reduces the expansion efficiency  $\eta_e$ . To analyze such under-expansion and over-expansion processes in the positive displacement expander, the following simple model was applied.

In the P–V diagram of the under-expansion process, the expansion work can be represented as the sum of the areas of the  $A_{1,u}$  and  $A_{2,u}$  regions.  $A_{1,u}$  can represent the enthalpy difference from isentropic expansion up to the design expansion pressure  $P_d$ , whereas  $A_{2,u}$  can represent the additional positive work  $(P_d - P_e)V_d$  occurring by blow-down due to the low back pressure. Therefore, the ideal expansion work  $\dot{W}_{u,id}$  during under-expansion can be given by:

$$\dot{W}_{u,id} = A_{1,u} + A_{2,u} = \dot{m}[(h_i - h_{d,s}) + (P_d - P_e)v_d] \quad (1)$$

where  $h_{d,s}$  represents the enthalpy during the isentropic expansion up to  $P_d$  and  $v_d$  refers to the specific volume of working fluid when expansion is completed (*i.e.*, just before the exhaust valve opens).

The ideal effective expansion efficiency  $\eta_{e,id}^*$  during under-expansion is the ratio of the ideal expansion work to the maximum work by isentropic expansion up to  $P_e$ :

$$\eta_{e,id}^* = \frac{\dot{W}_{u,id}}{\dot{m}(h_i - h_{e,s})} = \frac{h_i - h_{d,s} + (P_d - P_e)v_d}{h_i - h_{e,s}} \quad (2)$$

The actual expansion work  $\dot{W}_u$  during under-expansion can be represented by incorporating the efficiency of the expander  $\eta_e$  as follows:

$$\dot{W}_u = \eta_e \dot{W}_{u,id} = \eta_e \dot{m}[(h_i - h_{d,s}) + (P_d - P_e)v_d] \quad (3)$$

The actual effective expansion efficiency  $\eta_e^*$  during under-expansion is the ratio of the actual expansion work during under-expansion to the maximum work by isentropic expansion up to  $P_e$ :

$$\eta_e^* = \frac{\dot{W}_u}{\dot{m}(h_i - h_{e,s})} = \frac{h_i - h_{d,s} + (P_d - P_e)v_d}{h_i - h_{e,s}} \eta_e \quad (4)$$

In the P–V diagram showing the over-expansion process, the expansion work can similarly be represented by the difference between the positive work of area  $A_{1,o} + A_{2,o}$ , which can represent the enthalpy difference from isentropic expansion up to  $P_d$ , and the negative work of  $A_{2,o} + A_{3,o}$  from  $(P_d - P_e)V_d$  due to the back pressure increase. Therefore, the ideal expansion work during over-expansion  $\dot{W}_{o,id}$  can be expressed as:

$$\dot{W}_{o,id} = A_{1,0} + A_{2,0} - (A_{2,0} + A_{3,0}) = \dot{m}[(h_i - h_{d,s}) - (P_e - P_d)v_d] \tag{5}$$

where  $h_{d,s}$  and  $v_d$  are the same as for the under-expansion case.  $h_{d,s}$  represents the enthalpy during the isentropic expansion up to  $P_d$ , and  $v_d$  refers to the specific volume of the working fluid when expansion is completed (*i.e.*, just before the exhaust valve opens).

Here,  $\eta_{e,id}^*$  during over-expansion is the ratio of the ideal expansion work during over-expansion to the maximum work by isentropic expansion up to  $P_e$ :

$$\eta_{e,id}^* = \frac{\dot{W}_{o,id}}{\dot{m}(h_i - h_{e,s})} = \frac{h_i - h_{d,s} - (P_e - P_d)v_d}{h_i - h_{e,s}} \tag{6}$$

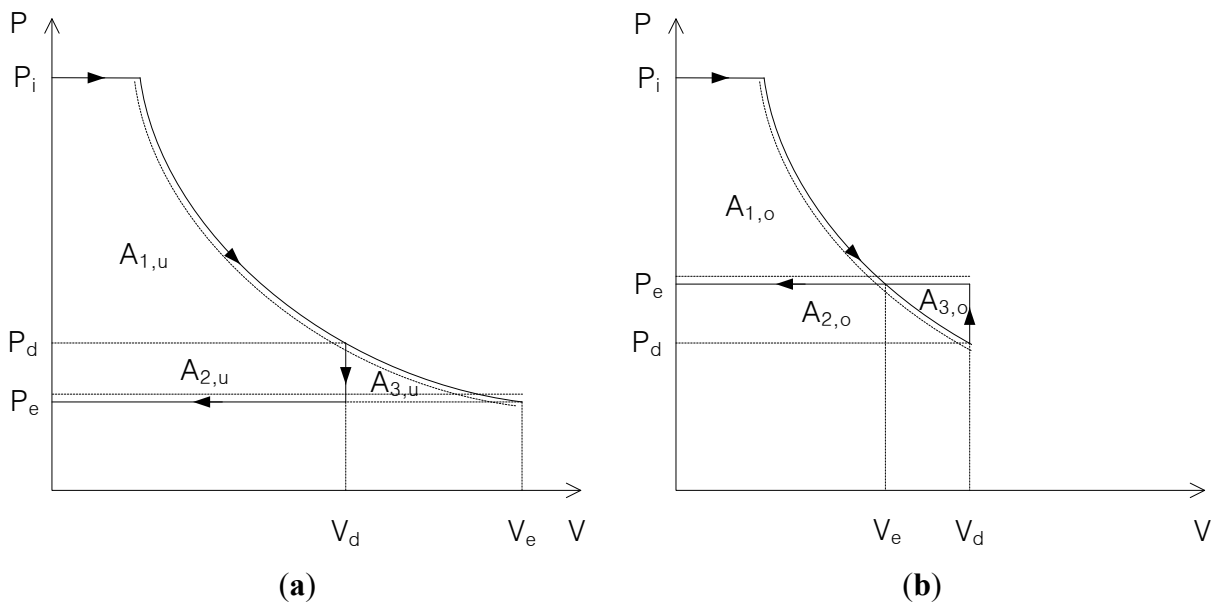
The actual expansion work during over-expansion  $\dot{W}_o$  can be represented by incorporating the efficiencies of expansion and compression  $\eta_e$  and  $\eta_c$ :

$$\dot{W}_o = \dot{m}[\eta_e(h_i - h_{d,s}) + (P_e - P_d)v_d/\eta_c] \tag{7}$$

Similar to the previous case,  $\eta_e^*$  during over-expansion is the ratio of the actual expansion work during over-expansion to the maximum work by isentropic expansion up to  $P_e$ :

$$\eta_e^* = \frac{\dot{W}_o}{\dot{m}(h_i - h_{e,s})} = \frac{\eta_e(h_i - h_{d,s}) - (P_e - P_d)v_d/\eta_c}{h_i - h_{e,s}} \tag{8}$$

**Figure 4.** Isentropic expansion process in the pressure–volume diagram: (a) under-expansion and (b) over-expansion.

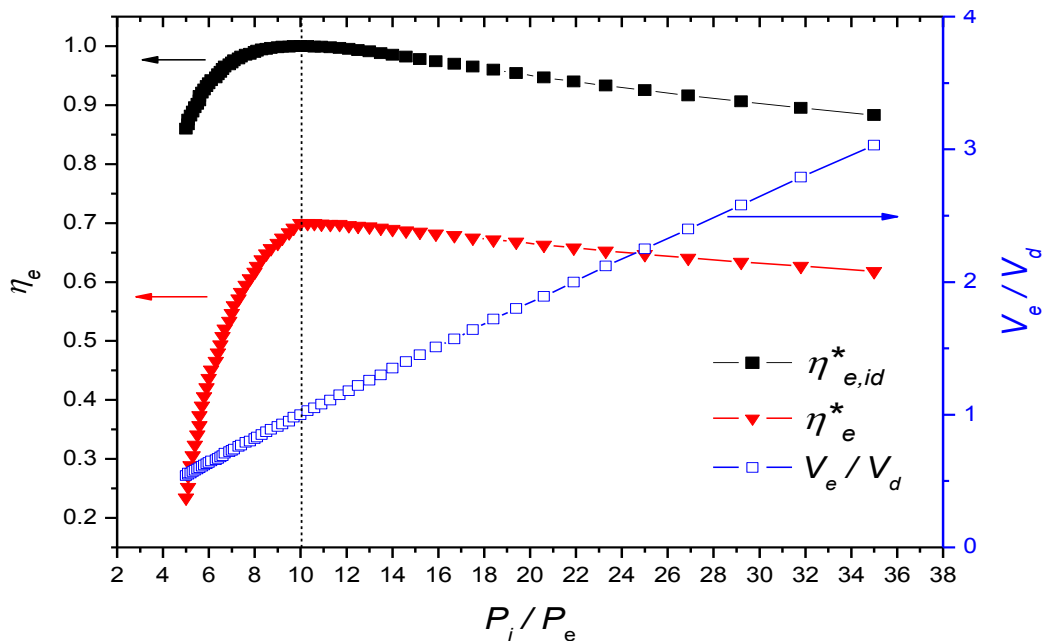


### 3.2. Characteristics of Expansion Efficiency during Under-Expansion and Over-Expansion

In [11], the design pressure ratio was set to 10 in consideration of the size of the swash plate-type expander in the HT cycle under the target operating conditions, while the condensation pressure and temperature were set to 3.5 bar and 139 °C, respectively. However, if  $T_{C,HT}$  is greater than the reference temperature of 139 °C, the design pressure ratio becomes higher than the actual operating pressure ratio, and over-expansion occurs. On the other hand, if  $T_{C,HT}$  is less than the reference temperature of 139 °C, the design pressure ratio becomes lower than the actual operating pressure

ratio, which results in under-expansion. Figure 4 shows the characteristics of the expander efficiency during under-expansion and over-expansion according to Equations (2), (4), (6), and (8) based on a design pressure ratio of 10 in the HT cycle. Assuming expansion and compression efficiencies  $\eta_c, \eta_e$  of 100% for the expander,  $\eta_{e,id}^*$  decreases by approximately 14% (absolute value) at an operating pressure ratio of 5 (*i.e.*, over-expansion) and by approximately 10% (absolute value) at an operating pressure ratio of 30 (*i.e.*, under-expansion). However, assuming expansion and compression efficiencies  $\eta_c, \eta_e$  of 70% for the expander,  $\eta_e^*$  decreases by approximately 47% (absolute value) at an operating pressure ratio of 5 and by approximately 7% (absolute value) at an operating pressure ratio of 30. When the actual expansion and compression efficiencies (70%) are applied to the P–V diagram in Figure 4, which assumes an isentropic process during under-expansion and over-expansion, the actual expansion work (*i.e.*, dash line) is less than the isentropic expansion work (*i.e.*, solid line), and the actual compression work (*i.e.*, dash line) is greater than the isentropic compression work (*i.e.*, solid line). Accordingly, the decrease in expansion efficiency is gradual during the under-expansion process because of the smaller loss of available work than the area of the region  $A_{3,u}$  (isentropic case). In contrast, the expansion efficiency decreased rapidly during the over-expansion process as more negative work is done than that represented by the area of the region  $A_{3,o}$  (isentropic case). The curve pattern of the effective expansion efficiency in Figure 5, which shows these off-design performance characteristics of the positive displacement expanders, is very similar to that of a more detailed model of a scroll expander [6].

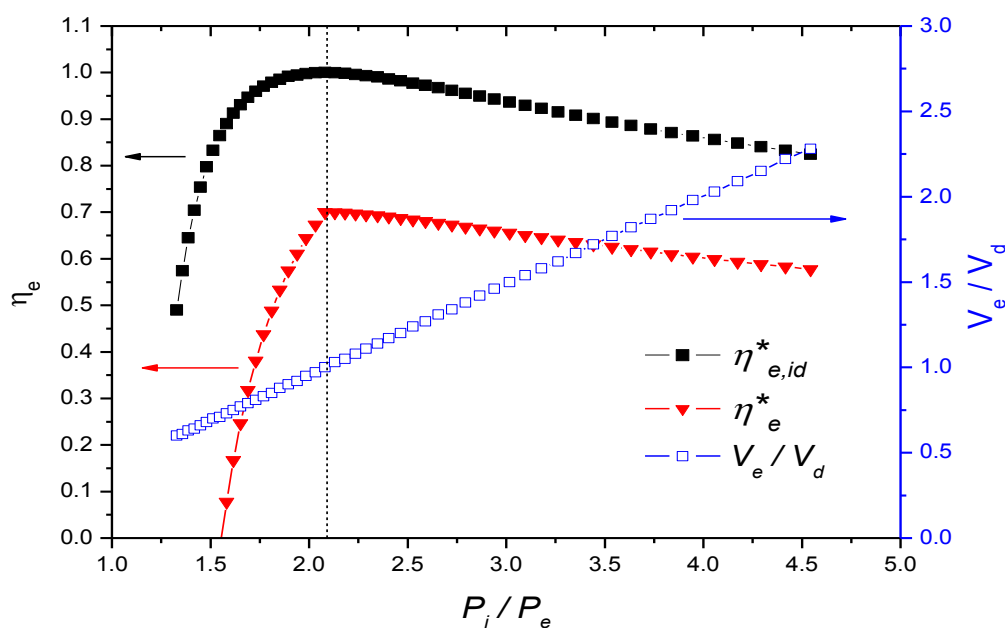
**Figure 5.** Effective expansion efficiency with imposed pressure ratio in the HT cycle.



For the LT cycle, the target operating condition was set to  $T_{CLT} = 40 \text{ }^\circ\text{C}$  (condensation pressure of 10.2 bar) with an ambient temperature of  $15 \text{ }^\circ\text{C}$  (*i.e.*, mean air temperature of all four seasons). However, it would be better for the positive displacement expander to be set to  $T_{CLT} = 60 \text{ }^\circ\text{C}$  (condensation pressure of 16.8 bar) at an ambient temperature of  $35 \text{ }^\circ\text{C}$  (*i.e.*, mean air temperature in summer) considering the highly gradual decrease in efficiency during under-expansion and rapid

decrease in efficiency during over-expansion as well as the size of expander. In that case, the expander can be run under over-expansion or under-expansion conditions if  $T_{C,LT}$  is higher or lower than the reference temperature of 60 °C in the actual LT cycle. Figure 6 shows the characteristics of the expander efficiency under under-expansion and over-expansion conditions based on a design pressure ratio of 2.08 in the LT cycle. Assuming expansion and compression efficiencies  $\eta_c, \eta_e$  of 100% for the expander,  $\eta_{e,id}^*$  decreased by approximately 51% (absolute value) at an operating pressure ratio of 1.33 under the over-expansion condition and by approximately 17% (absolute value) at an operating pressure ratio of 4.54 under an under-expansion condition. However, assuming expansion and compression efficiencies  $\eta_c, \eta_e$  of 70% for the expander,  $\eta_e^*$  became  $-126\%$  (absolute value) at an operating pressure ratio of 1.33 under the over-expansion condition. This acted as a load because the negative work was actually increased. On the other hand, the expansion efficiency decreased by approximately 12% (absolute value) at an operating pressure ratio of 4.54 under the under-expansion condition.

**Figure 6.** Effective expansion efficiency with imposed pressure ratio in the LT cycle.



#### 4. Performance Model of Engine Waste Heat Recovery System According to Operating Conditions

##### 4.1. Effect of HT Cycle Condensation Temperature

Table 1 presents two cases for the operation characteristics of the HT cycle: (A) when the design pressure ratio  $P_{r,d}$  of the expander was set to 10, 17.5, and 29.2 (corresponding to a design volume ratio  $V_{r,d}$  of 7.4, 12.3, and 29.2, respectively) in accordance with the decreasing  $T_{C,HT}$  (the design pressure ratio  $P_{r,d}$  was equal to the operating pressure ratio  $P_r$  here); and (B) the under-expansion state when  $P_{r,d}$  and  $V_{r,d}$  were set to 10 and 7.4, respectively, and  $P_r$  was set to 10, 17.5, and 29.2 as  $T_{C,HT}$  decreased.

In case A, when  $P_{r,d}$  was increased from 10 to 17.5 to 29.2 (to have the same value as  $P_r$ ), the HT cycle output increased by 21% and 38%, respectively, as  $T_{C,HT}$  decreased in comparison to the output

at a design/operating pressure ratio of 10. However, as the design pressure ratio increased, the volume of the expander increased by 64% and then by 158% (for  $P_{r,d} = 29.2$ ) in comparison to the volume of the expander at the design/operating pressure ratio of 10. In case B, when  $P_r$  was increased from 10 to 17.5 to 29.5,  $P_{r,d}$  was fixed at 10, and  $T_{C,HT}$  decreased, the HT cycle output increased by 17% and 25%, respectively, in comparison to the output at  $P_r$  of 10 based on  $\eta_e^*$  under the off-design conditions in Figure 5.

Based on the above analysis results, the target operating conditions of the HT cycle should be set to under-expansion.  $P_{r,d}$  and  $V_{r,d}$  of the expander should be set to 10 and 7.4, respectively, while the operating pressure ratio  $P_r$  should be set to 29.2 as  $T_{C,HT}$  is decreased to 104.8 °C in order to improve the HT cycle output. This will reduce the volume and weight of the expander to less than half (approximately 39%) despite an approximately 7% decrease in the expander efficiency  $\eta_e^*$ .

**Table 1.** Operation characteristics of the high-temperature (HT) cycle (A) with varying expander  $P_{r,d}$  ( $=P_r$ ) and decreasing  $T_{C,HT}$  and (B) for the under-expansion state with  $P_{r,d}$  fixed to 10, varying  $P_r$ , and decreasing  $T_{C,HT}$ .

Case	$P_{C,HT}$ (bar)	$T_{C,HT}$ (°C)	$P_{r,d}$ ( $V_{r,d}$ )	$P_r$	$\frac{V_e}{V_d}$	$\frac{\eta_e}{\eta_e^*}$	$\dot{m}_r$ (g/s)	$\dot{W}_P^+$ (kW)	$\dot{W}_E^-$ (kW)	$\dot{W}_{net}^+$ (kW)	$\eta_{th}$ (%)
A	2.0	138.9	10(7.4)	10	1.00	0.7	8.6	0.04	2.69	2.65	13.0
	1.2	120.2	17.5(12.3)	17.5	1.00	0.7	8.6	0.04	3.25	3.21	15.1
	3.5	104.8	29.2(19.6)	29.2	1.00	0.7	8.6	0.04	3.71	3.67	16.8
B	2.0	138.9	10(7.4)	10	1.00	0.7	8.6	0.04	2.69	2.65	13.0
	1.2	120.2	10(7.4)	17.5	1.64	0.675	8.6	0.04	3.14	3.10	14.6
	3.5	104.8	10(7.4)	29.2	2.58	0.634	8.6	0.04	3.36	3.32	15.2

#### 4.2. Effect of LT Cycle Condensation Temperature

Table 2 presents two cases for the operation characteristics of the LT cycle: (A) when  $P_{r,d}$  of the expander was set to 2.1, 2.7, 3.4, and 4.5 (corresponding to a design volume ratio  $V_{r,d}$  of 2.4, 3.2, 4.2, and 5.7, respectively), in accordance with a decreasing  $T_{C,HT}$  (the design pressure ratio  $P_{r,d}$  was equal to the operating pressure ratio  $P_r$  here); and (B) an under-expansion state when  $P_{r,d}$  and  $V_{r,d}$  were fixed to 2.1 and 2.4, respectively, and  $P_r$  was set to 2.1, 2.7, 3.4, and 4.5, as  $T_{C,LT}$  was decreased.

In case A, when  $P_{r,d}$  was increased from 2.1 to 2.7, 3.4, and 4.5 (to have the same value as  $P_r$ ) as  $T_{C,LT}$  decreased, the LT cycle output increased by 32%, 61%, and 90%, respectively, compared to the LT cycle output at a design/operating pressure ratio of 2.1. However, as the design pressure ratio increased, the volume of the expander had to be increased by 19%, 49%, and 79%, respectively, in comparison to the volume of the expander at the design/operating pressure ratio of 2.1.

In case B, when  $P_r$  was increased from 2.1 to 2.7, 3.4, and 4.5,  $P_{r,d}$  and  $V_{r,d}$  were fixed to 2.1 and 2.4, respectively, as  $T_{C,LT}$  decreased. The LT cycle output increased by 26%, 42%, and 51%, respectively, in comparison to the LT cycle output at a  $P_r$  of 2.1 with  $\eta_e^*$  under the off-design conditions given in Figure 6.

$T_{C,LT}$  of the LT cycle can vary significantly depending on the outdoor temperature of the air-cooled condenser and heat exchanger performance. For the LT expander, the design pressure and volume

ratios should be set at 2.1 and 2.4, respectively, with  $T_{C,LT} = 60$  °C (condensation pressure of 16.8 bar). This is based on the mean air temperature in the summer season of 35 °C, the very gradual decrease in the expander efficiency during under-expansion and rapid decrease in the expander efficiency during over-expansion, and the size of expander. In this case, although the expander efficiency decreased by approximately 7% under  $T_{C,LT} = 40$  °C because of the off-design operation, the volume and weight of the expander were reduced by approximately 33% compared to when the design pressure ratio was 3.4 for  $T_{C,LT} = 40$  °C (condensation pressure of 10.2 bar). This would be advantageous because it can prevent a rapid decrease in the expander efficiency due to over-expansion from the typical increase in air temperature during the summer season.

**Table 2.** Operation characteristics of the LT cycle (A) with varying expander  $P_{r,d} (=P_r)$  and decreasing  $T_{C,LT}$  and (B) for the under-expansion state with  $P_{r,d}$  fixed to 2.1, varying  $P_r$ , and decreasing  $T_{C,LT}$ .

Case	$P_{C,HT}$ (bar)	$T_{C,HT}$ (°C)	$P_{r,d} (V_{r,d})$	$P_r$	$\frac{V_e}{V_d}$	$\frac{\eta_e}{\eta_e^*}$	$\dot{m}_r$ (g/s)	$\dot{W}_P^+$ (kW)	$\dot{W}_E^-$ (kW)	$\dot{W}_{net}^+$ (kW)	$\eta_{th}$ (%)
A	16.8	60.0	2.1(2.4)	2.1	1.00	0.7	271.1	0.54	2.49	1.95	4.7
	13.2	50.0	2.7(3.2)	2.7	1.00	0.7	252.8	0.63	3.20	2.57	6.1
	10.2	40.0	3.4(4.2)	3.4	1.00	0.7	231.8	0.62	3.75	3.14	7.5
	7.7	30.0	4.5(5.7)	4.5	1.00	0.7	214.6	0.61	4.32	3.71	8.8
B	16.8	60.0	2.1(2.4)	2.1	1.00	0.7	271.1	0.54	2.49	1.95	4.7
	13.2	50.0	2.1(2.4)	2.7	1.19	0.677	252.8	0.63	3.09	2.46	5.9
	10.2	40.0	2.1(2.4)	3.4	1.49	0.631	231.8	0.62	3.38	2.76	6.6
	7.7	30.0	2.1(2.4)	4.5	1.79	0.577	214.6	0.61	3.56	2.95	7.0

## 5. Conclusions

The performance of a positive displacement expander in a dual-loop engine waste heat recovery system currently under development in South Korea was analyzed at different design pressure ratios. Because the expander in a vehicle waste heat recovery system may be required to operate in an under-expansion or over-expansion state depending on the operating conditions, the predicted performance under off-design conditions is highly important. Furthermore, not only the expansion efficiency but also the volume and weight of the expander are highly important to the expander design. Accordingly, optimization of the design pressure ratio must take into account all of these factors. To achieve this goal, a simple model was developed to predict the performance of the positive displacement expander under under-expansion or over-expansion operating conditions, and the expansion performance and cycle analysis under off-design conditions were analyzed. In the results, a gradual decrease in the expansion efficiency was observed during under-expansion operation (*i.e.*, the design pressure ratio is lower than the operating pressure ratio), whereas a rapid decrease in the expansion efficiency was apparent during over-expansion operation (*i.e.*, the design pressure ratio is higher than the operating pressure ratio).

Based on the above analysis results, the HT cycle should be set to function in an under-expanded state: the design pressure ratio  $P_{r,d}$  and corresponding design volume ratio  $V_{r,d}$  of the expander should be set to 10 and 7.4, respectively, while the operating pressure ratio  $P_r$  should be set to 29.2 by decreasing the condensation temperature  $T_{C,HT}$  to 104.8 °C. This will improve the HT cycle output while reducing the volume and weight of the expander to less than half (approximately 39%) despite a decrease in the expansion efficiency of approximately 7%.

In the LT cycle, the condensation temperature  $T_{C,LT}$  can vary significantly depending on the outdoor temperature of the air-cooled condenser and the heat exchanger performance. The LT expander should be set to a design pressure ratio and corresponding design volume ratio of as low as 2.1 and 2.4, respectively, with a condensation temperature  $T_{C,LT}$  of 60 °C (condensation pressure of 16.8 bar) based on 35 °C, which is the mean air temperature in summer. This is because of the very gradual decrease in the expansion efficiency during under-expansion and the rapid decrease in the expander efficiency during over-expansion as well as the size of the expander. Although operating under a condensation temperature  $T_{C,LT}$  of 40 °C may decrease the expansion efficiency by approximately 7% because of the off-design operation, the volume and weight of the expander can be reduced by approximately 33% compared to when the design pressure ratio and corresponding design volume ratio are 3.4 and 4.2, respectively, with a condensation temperature  $T_{C,LT}$  of 40 °C (condensation pressure of 10.2 bar). Furthermore, this would prevent the rapid decrease in the expansion efficiency due to over-expansion from the typical increase in the air temperature during the summer.

### Author Contributions

All authors contributed to this paper. Young-Min Kim designed the simulations. Dong-Gil Shin and Chang-Gi Kim discussed the results and implications together and commented on the manuscript at all stages.

### Nomenclature

$h$	specific enthalpy (kJ/kg)
$\dot{m}$	mass flow rate (kg/s)
$P$	pressure (kPa)
$P_r$	pressure ratio
$V_r$	volume ratio
$Q$	volume ratio
$\dot{Q}$	rate of heat transfer (kW)
$T$	temperature (K)
$V$	volume (m <sup>3</sup> )
$v$	specific volume (m <sup>3</sup> /kg)
$\dot{W}$	rate of work (kW)

### Greek symbols

$\eta_c$	compression efficiency
$\eta_e, \eta_e^*$	expansion efficiency, effective expansion efficiency
$\eta_{th}$	thermal efficiency

## Subscripts

C	condensing
CW	cooling water
<i>d</i>	design
<i>E, e</i>	expansion
HT	high temperature cycle
<i>i, e</i>	inlet, exit
id	ideal process
LT	low temperature cycle
net	net work
P	pump
<i>r</i>	refrigerant
<i>s</i>	isentropic process
<i>u, o</i>	under-expansion, over-expansion

## Conflicts of Interest

The authors declare no conflict of interest.

## References

1. Dolz, V.; Novella, R.; Garcia, A.; Sanchez, J. HD Diesel engine equipped with a bottoming Rankine cycle as a waste heat recovery system. Part 1: Study and analysis of the waste heat recovery. *Appl. Therm. Eng.* **2012**, *36*, 269–278.
2. Wang, E.H.; Zhang, H.G.; Zhao, Y.; Fan, B.Y.; Wu, Y.T.; Mu, Q.H. Performance analysis of a novel system combining a dual loop organic Rankine cycle (ORC) with a gasoline engine. *Energy* **2012**, *43*, 385–395.
3. Vaja, I.; Gambarotta, A. Internal combustion engine (ICE) bottoming with organic Rankine cycles (ORCs). *Energy* **2010**, *35*, 1084–1093.
4. Heo, H.S.; Bae, S.J. Technology trends of Rankine steam cycle for engine waste heat recovery. *Auto J. KSAE* **2010**, *32*, 23–32.
5. Kim, H.J.; Kim, H.J. Design of a swash plate-type of steam expander for waste heat recovery. *Korean J. Air-Cond. Refrig. Eng.* **2011**, *23*, 313–320.
6. Lemort, V.; Quoilin, S.; Cuevas, C.; Lebrun, J. Testing and modeling a scroll expander integrated into an organic Rankine cycle. *Appl. Therm. Eng.* **2009**, *29*, 3094–3102.
7. Bae, S.; Heo, H.; Lee, H.; Lee, D.; Kim, T.; Park, J.; Kim, C. Performance characteristics of a steam cycle and boiler for engine waste heat recovery. *SAE Tech. Pap.* **2011**, *2011*, doi:10.4271/2011-28-0055.
8. Ringler, J.; Seifert, M.; Guyotot, V.; Hübner, W. Rankine cycle for waste heat recovery of IC engines. *SAE Tech. Pap.* **2009**, *2009*, doi:10.4271/2009-01-0174.

9. Tchanche, B.F.; Lambrinos, G.; Frangoudakis, A.; Papadakis, G. Low-grade heat conversion into power using organic Rankine cycles—A review of various applications. *Renew. Sustain. Energy Rev.* **2011**, *15*, 3963–3979.
10. Zanelli, R.; Favrat, D. Experimental Investigation of a Hermetic Scroll Expander-Generator. In Proceedings of the International Compressor Engineering Conference, Purdue University, West Lafayette, IN, USA, 19–22 July 1994; p. 1021.
11. Kim, Y.M.; Shin, D.G.; Kim, C.G.; Woo, S.J.; Choi, B.C. Performance analysis of two-loop Rankine cycle for engine waste heat recovery. *J. Energy Eng.* **2012**, *21*, 398–406.

© 2014 by the authors; licensee MDPI, Basel, Switzerland. This article is an open access article distributed under the terms and conditions of the Creative Commons Attribution license (<http://creativecommons.org/licenses/by/3.0/>).